

Nicole K. Polinski¹, Terina N. Martinez¹, An Phu Tran Nguyen², Darren Moore², Samuel Young³, Alexia Kalogeropoulou⁴, Dario Alessi⁴, Shalini Padmanabhan¹, Marco Baptista¹, Kuldip D. Dave¹
The Michael J. Fox Foundation for Parkinson's Research¹, Van Andel Research Institute², University of Iowa³, University of Dundee⁴

Introduction

As the greatest known genetic contributor to Parkinson's disease (PD), the leucine-rich repeat kinase 2 (LRRK2) gene and protein are targets of interest for Parkinson's disease research and therapeutic development. Unfortunately, critical research tools for understanding the function and role of LRRK2 in disease pathogenesis are lacking. To address this gap, The Michael J. Fox Foundation (MJFF) has taken an active role in designing, validating, and distributing various tools and models that can be used to investigate LRRK2-related mechanisms of PD neurodegeneration or strategies to prevent, slow, or halt disease progression. Here we summarize MJFF-led efforts to develop and characterize a variety of LRRK2-related tools. One such tool is a set of viral vectors that can be used to overexpress wild-type and various mutant forms of LRRK2 *in vivo* to understand the role of this protein in disease biology, pathways related to PD, and test therapeutic interventions aimed at reducing LRRK2-related pathology. Characterization data for these viral vectors in the rat brain will be presented, including information on the expression profile and resulting neurodegeneration. In addition, we will be presenting data on a new mouse model that overexpresses Rab29 protein—a protein that increases LRRK2 kinase activity and act as a substrate for LRRK2 kinase activity. We will provide data on the protein and mRNA expression levels, as well as data demonstrating the effects on LRRK2 kinase activity. Finally, we will include information on how to access these important tools and models. Ultimately, MJFF's investment in providing the research community with robust, well-characterized tools and models will speed research towards a cure for PD by enabling research, de-risking investment in PD research, and increasing reproducibility by providing the tools to researchers across labs.

LRRK2-Overexpression Viral Vectors for *In Vivo* Use

MJFF generated viral vectors expressing 3xFLAG-tagged LRRK2 (WT, G2019S, or G2385R) and 3xFLAG-tagged thymidine kinase (TK) for use *in vivo*. Expression is driven by the human synapsin promoter. Viral vectors were designed and generated by Dr. Samuel Young at the University of Iowa, characterized by Dr. Darren Moore at the Van Andel Research Institute, and are available at the University of Iowa Vector Core. A summary of the viral vector properties and *in vivo* performance in the rat brain is described herein.

	Particle Count	RCA Probe -E1a For Virus Copies	Viral Particle: Infectious Unit	HdAd Infectivity	Helper Virus Contamination	University of Iowa Product Number
HdAd5 - Syn - 3XFLAG TK	7.54E+12 vp/mL	0 virus/mL	142 VP:IU	5.32E+10 IU/mL	0.03%	VVC-MJFF-7337
HdAd5 - Syn - 3XFLAG WT LRRK2	6.94E+12 vp/mL	0 virus/mL	103 VP:IU	6.76E+10 IU/mL	0.04%	VVC-MJFF-7334
HdAd5 - Syn - 3XFLAG G2019S LRRK2	4.08E+12 vp/mL	0 virus/mL	76 VP:IU	5.38E+10 IU/mL	0.05%	VVC-MJFF-7335
HdAd5 - Syn - 3XFLAG G2385R LRRK2	5.63E+12 vp/mL	0 virus/mL	90 VP:IU	6.26E+10 IU/mL	0.04%	VVC-MJFF-7336

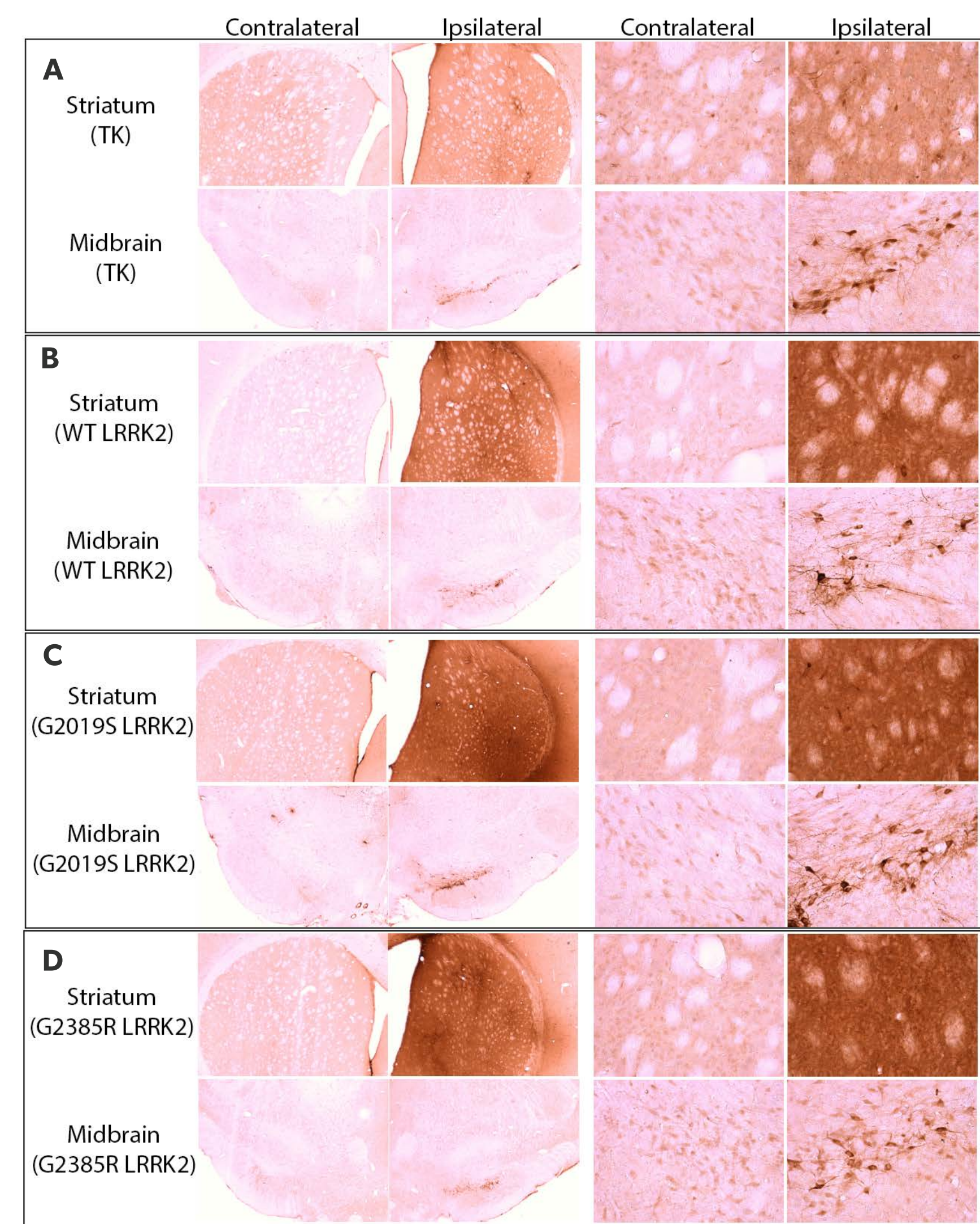


Figure 1. HdAd5 transgene expression in the striatum and midbrain at 42 days post-intra-striatal injection. Representative images taken from anti-FLAG immunostained sections of the striatum and ventral midbrain from adult female Wistar rats injected with HdAd5 viral vectors at 4.2x10⁹ vp/site (in 2ul) at six intra-striatal injection sites in a single coronal plane. Low magnification images of the injected (ipsilateral) and uninjected (contralateral) hemispheres appear on the left. High magnification images of the ipsilateral and contralateral hemispheres appear on the right. Injection of HdAd5-Syn-3XFLAG TK (A), HdAd5-Syn-3XFLAG WT LRRK2 (B), HdAd5-Syn-3XFLAG G2019S LRRK2 (C), and HdAd5-Syn-3XFLAG G2385R LRRK2 (D) resulted in robust expression, as detected using the FLAG tag, throughout the injected striatum as well as within the dopaminergic cell bodies in the substantia nigra pars compacta in the midbrain.

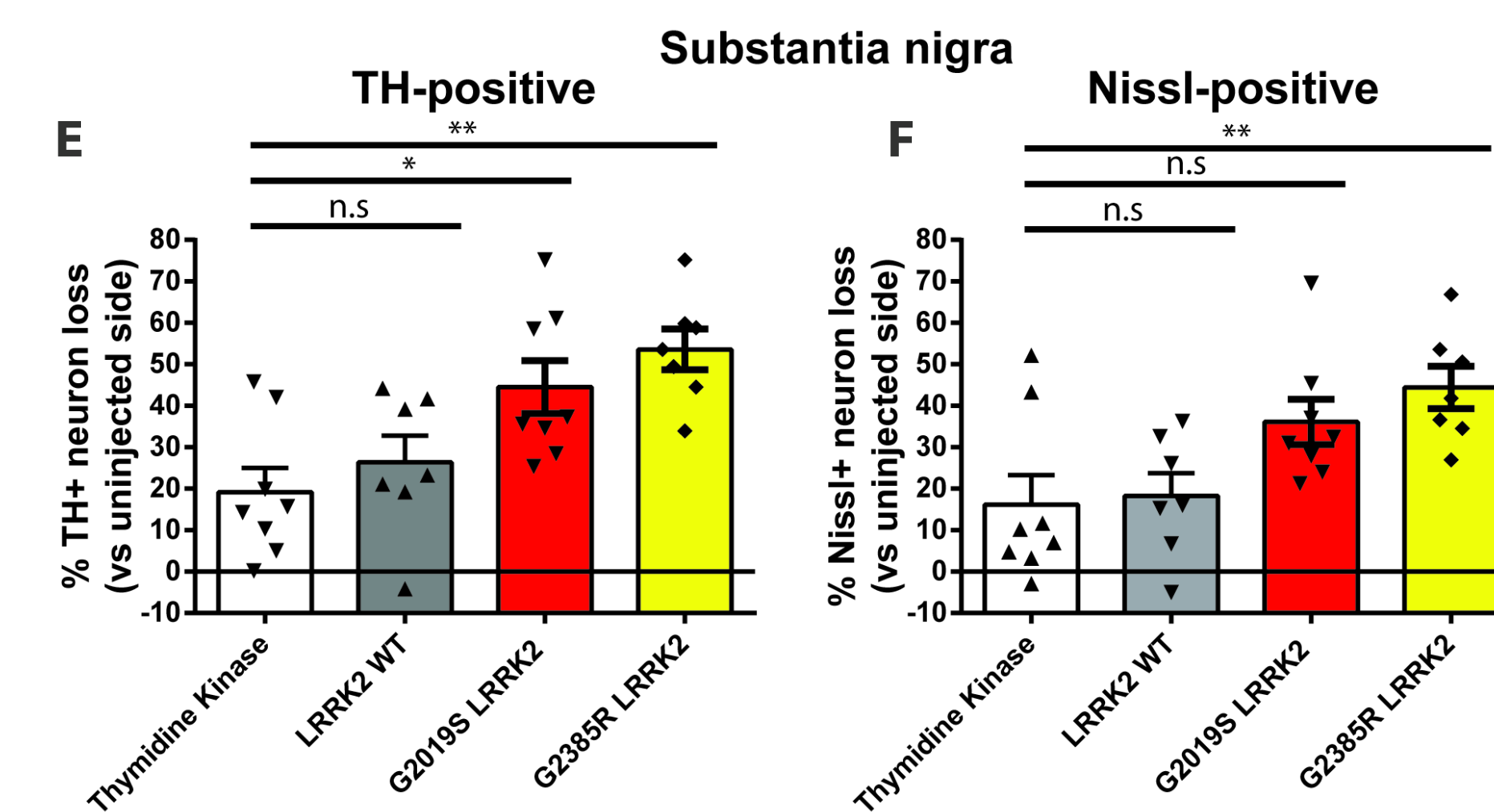
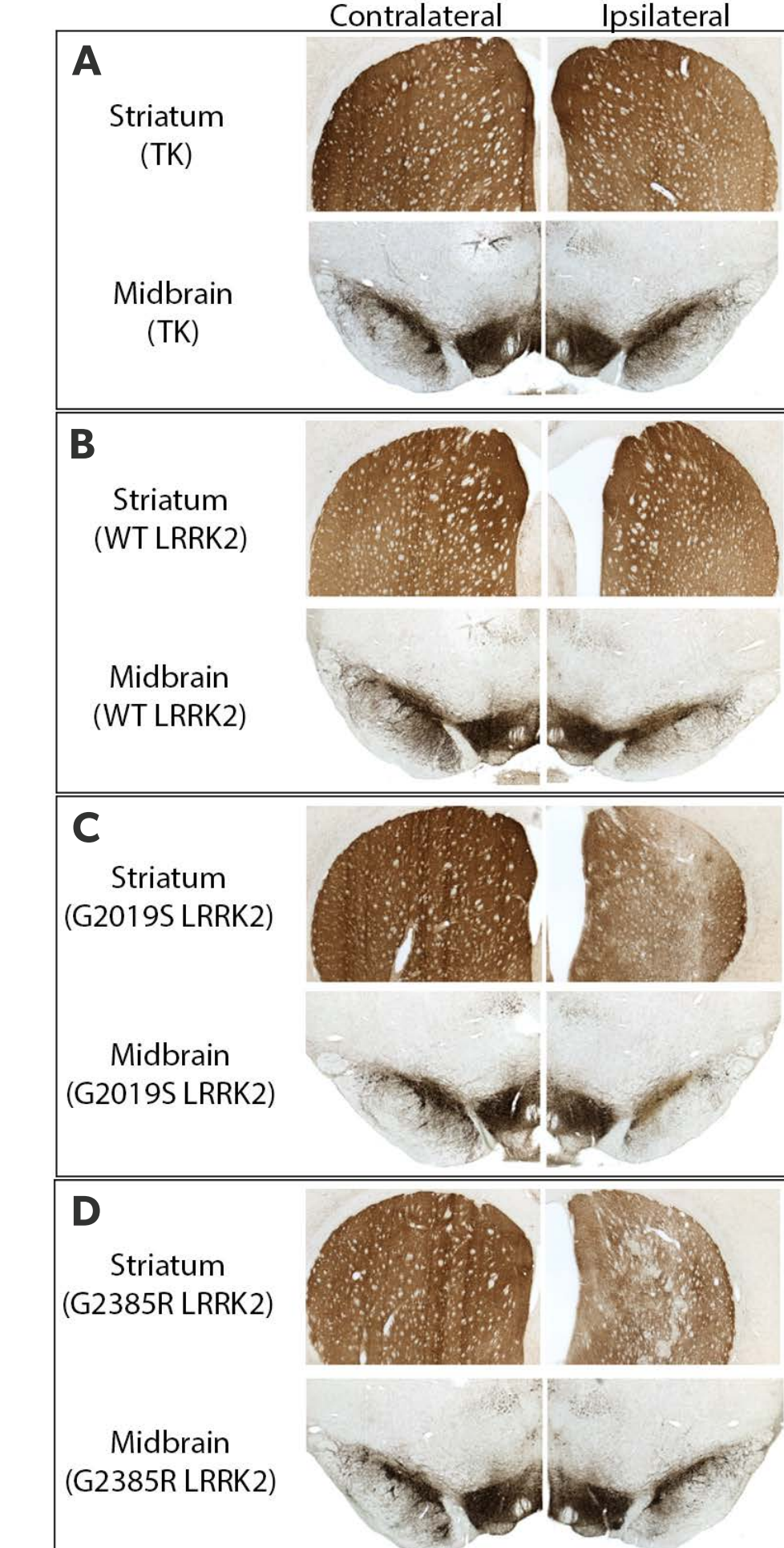


Figure 2. Nigrostriatal degeneration resulting from intra-striatal injection of HdAd5 LRRK2- or TK-expressing viral vectors at 42 days post-injection. A-D) Representative images taken from tyrosine hydroxylase (TH) immunostained sections of the striatum and midbrain from rats injected with HdAd5 viral vectors at 4.2x10⁹ vp/site at six intra-striatal injection sites. E-F) Stereological quantitation of TH-positive and Nissl-positive cells in the ipsilateral substantia nigra pars compacta, represented as percent loss from the contralateral hemisphere. Injection of HdAd5-Syn-3XFLAG TK and HdAd5-Syn-3XFLAG WT LRRK2 result in minimal non-specific degeneration at 42 days post-injection (A, B, E, F) whereas HdAd5-Syn-3XFLAG G2019S LRRK2 and HdAd5-Syn-3XFLAG G2385R LRRK2 result in ~44% and ~53% loss of nigral dopaminergic neurons, respectively, and loss of striatal nerve terminals (C-F). Bars represent mean ± SEM (n=8/group). * P<0.05 or ** P<0.01, by one-way ANOVA with Bonferroni's post-hoc test.

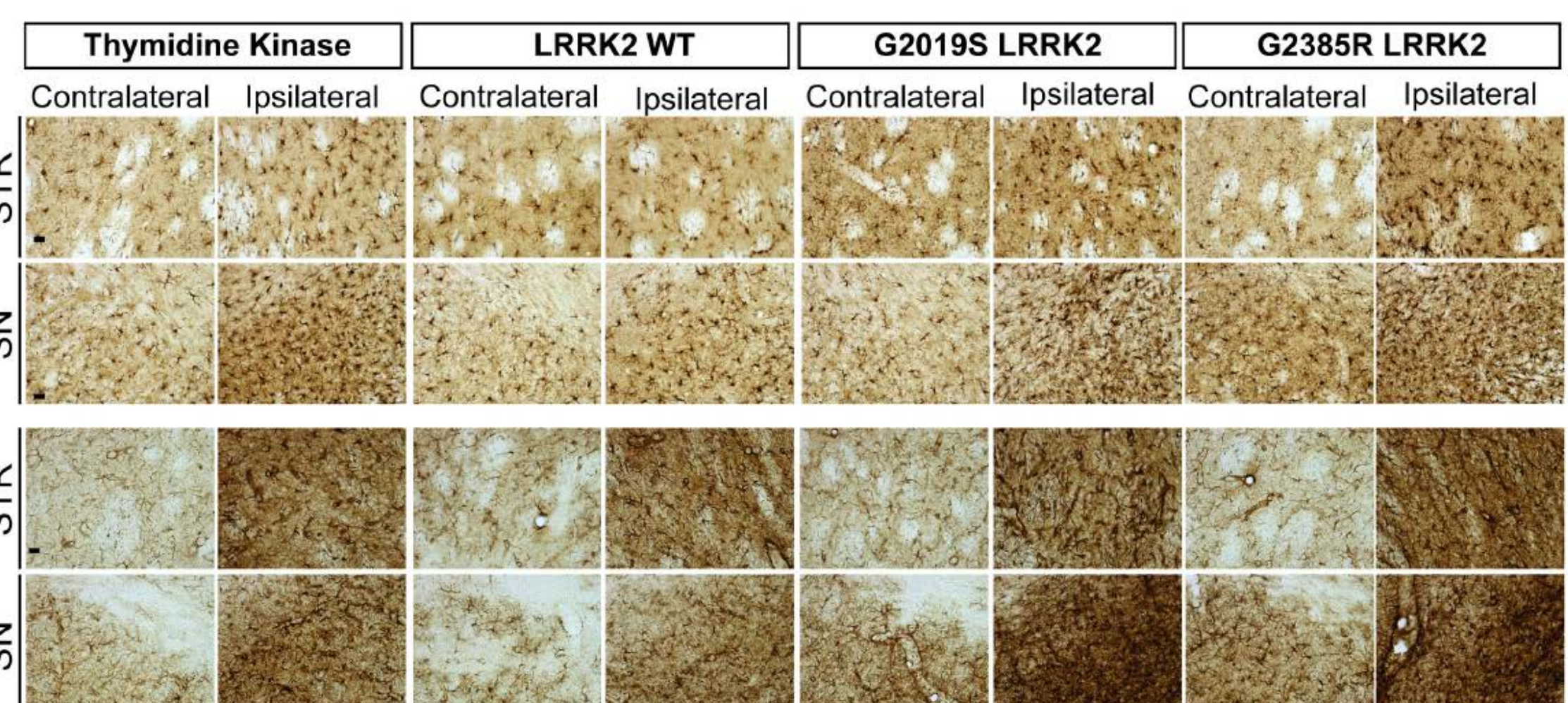


Figure 3. Robust neuroinflammation in the nigrostriatal pathway at 42 days post-intra-striatal injection. Representative images taken from anti-Iba1 and anti-GFAP immunostained sections of the striatum and ventral midbrain from adult female Wistar rats injected with HdAd5 viral vectors at 4.2x10⁹ vp/site (in 2ul) at six intra-striatal injection sites in a single coronal plane. Injection of all HdAd5 viral vectors resulted in increased microglial and astrocyte inflammation markers, with potentially greater astrogliosis following HdAd5-Syn-3XFLAG G2019S LRRK2 and HdAd5-Syn-3XFLAG G2385R LRRK2.

Rab29 Overexpression Mouse Model

MJFF generated a new mouse model overexpressing the murine *Rab29* gene to enable further investigation into the role of Rab29 in PD and relationship of this protein to other PD-related proteins like LRRK2. The line was generated at Taconic Biosciences where it is now distributed. Characterization of Rab29 expression and effect on LRRK2 activity was performed by Dr. Dario Alessi at the University of Dundee.

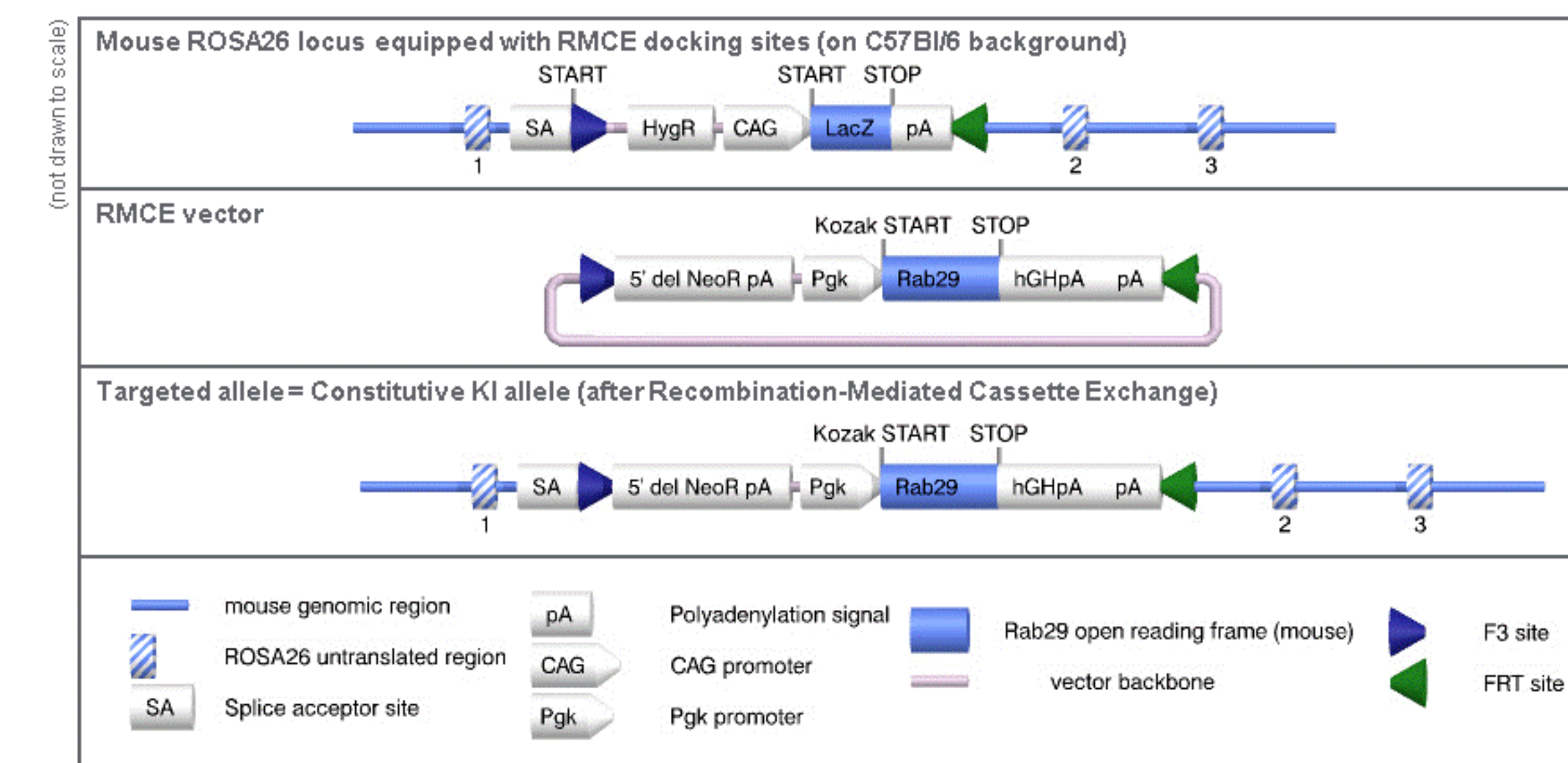


Figure 4. Targeting and transgene schematic for generation of the Rab29 overexpression mouse model. The mouse *Rab29* open reading frame was inserted into the RMCE vector, with expression driven by the Pkg promoter. The vector was inserted into the ROSA26 locus through recombination-mediated cassette exchange to produce a constitutive knock-in.

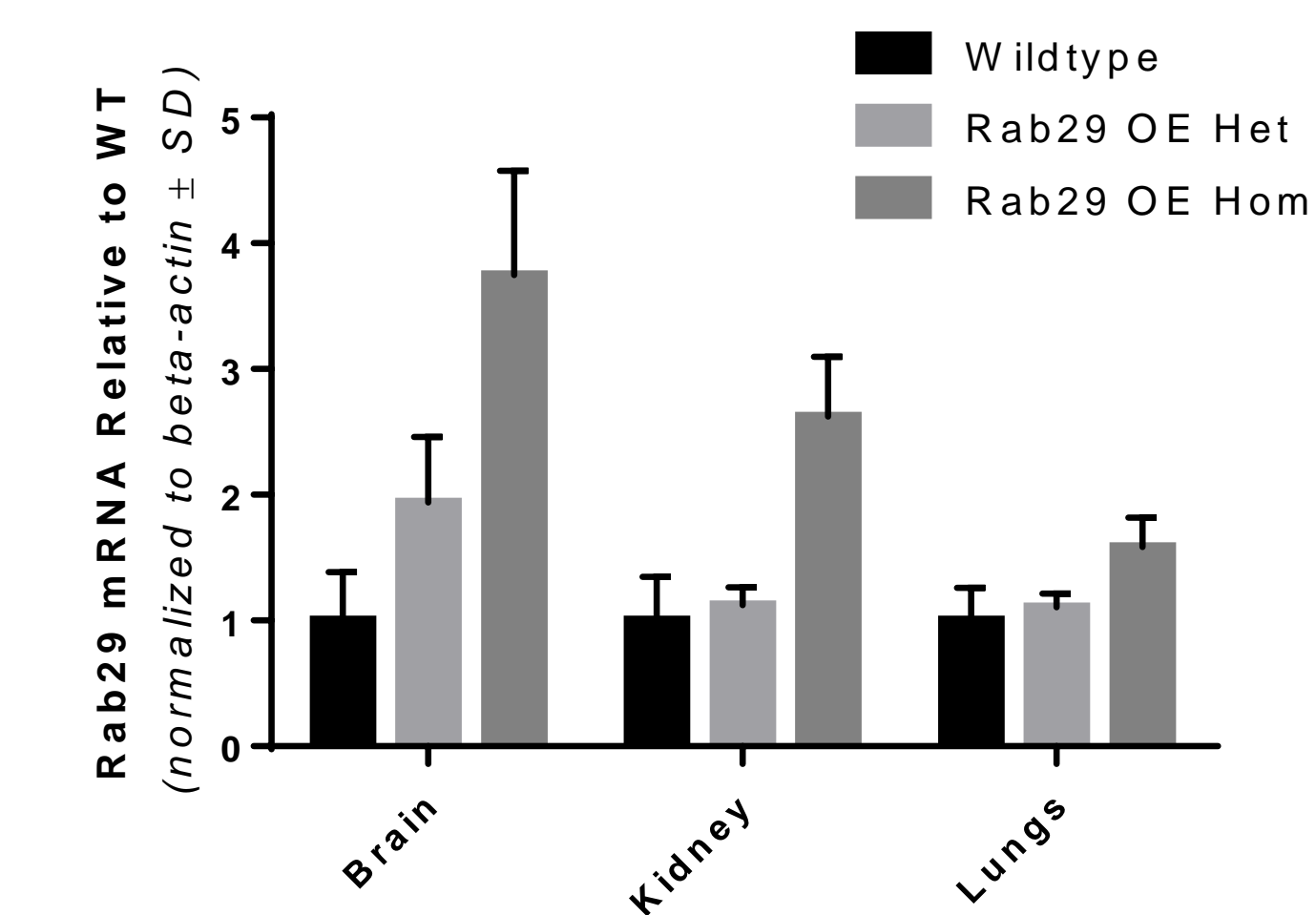


Figure 5. Rab29 mRNA Expression is differentially increased in the Rab29 heterozygous and homozygous mice in brain, kidney, and lungs. Data was obtained through qPCR for mouse *Rab29* with beta actin as the housekeeping gene. Four biological replicates per genotype at three months of age, and two technical replicates per reaction were run (technical replicates were averaged). Brain levels of *Rab29* mRNA were ~1.9 fold increased in the *Rab29* OE Het mice and ~3.7 fold increased in the *Rab29* OE Hom mice. Kidney levels of *Rab29* mRNA were unchanged in the *Rab29* OE Het mice and ~2.6 fold increased in the *Rab29* OE Hom mice. Lung levels of *Rab29* mRNA unchanged in the *Rab29* OE Het mice and ~1.6 fold increased in the *Rab29* OE Hom mice. Bars represent mean ± standard deviation.

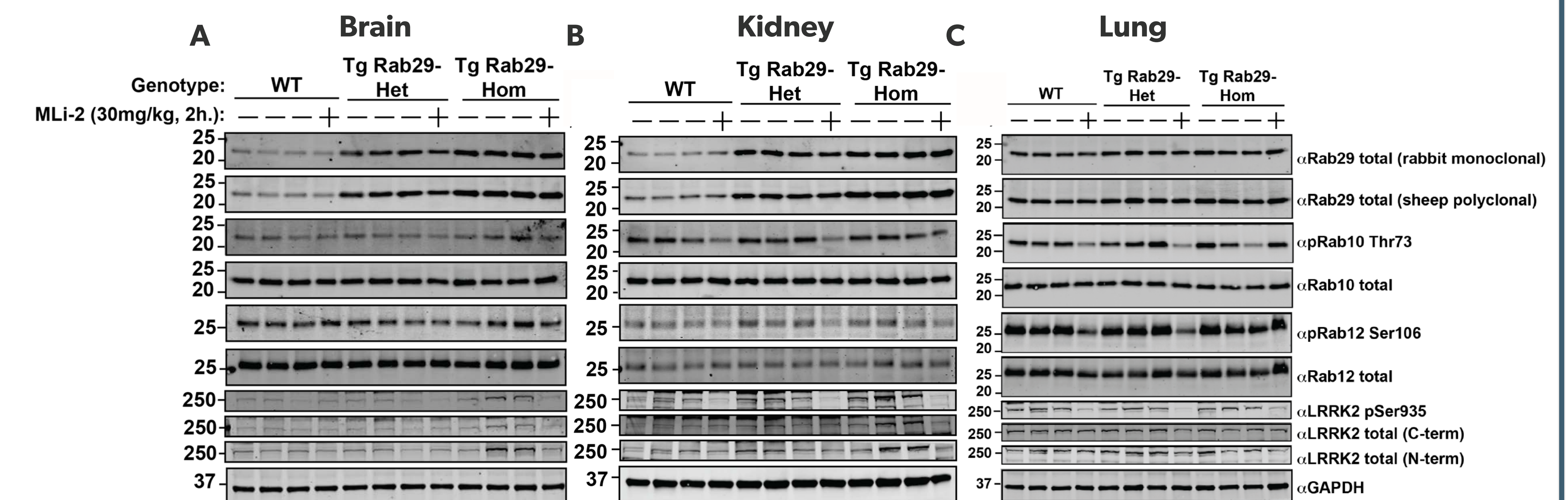


Figure 6. Rab29 Protein Expression is differentially increased in the Rab29 heterozygous and homozygous mice in brain, kidney, and lungs with no changes observed in measures of LRRK2 kinase activity. Protein levels of total Rab29 protein, total Rab 10 protein, pT73 Rab 10 protein, total Rab 12 protein, pS106 Rab12 protein, total LRRK2, and pS935 LRRK2, GAPDH were assessed in whole tissue homogenates of (A) Brain, (B) Kidney, and (C) Lung from wildtype, *Rab29* OE Het mice, and *Rab29* OE Hom mice at three months of age. Total *Rab29* protein levels are shown in the top two rows of bands, using two different antibodies to the *Rab29* protein. *Rab29* protein is increased in *Rab29* OE Het and Hom mouse brain and kidney as compared to wildtype. *Rab29* protein does not appear to be significantly increased in the *Rab29* OE Het and Hom mouse lung. Measures of LRRK2 kinase activity were also included. These include pT73 Rab 10 (with total Rab 10 protein for normalization), pS106 Rab12 (with total Rab12 for normalization), and pS935 LRRK2 (with total LRRK2 protein for normalization). To confirm the ability to modulate LRRK2 kinase activity and see subsequent reduction in substrate phosphorylation or autophosphorylation, one animal was treated with MLI-2. *Rab29* OE Het and Hom mice do not display detectable increase in endogenous LRRK2 kinase activity in any tissue. GAPDH was used as the loading control.

Summary and More Information

MJFF is invested in providing the PD research community with high-quality tools and models to support rapid new discoveries and encourage reliable, reproducible data. The tools described in this poster are the result of recent collaborative efforts aimed at generating molecular tools and animal models for LRRK2-related research in particular. Information on other LRRK2 tools or tools for other PD-related targets can be found in the Research Tools Catalog at www.michaeljfox.org/toolscatalog. Questions regarding MJFF preclinical tools can be sent to tools@michaeljfox.org. In addition, MJFF also offers patient biosamples (eg blood, CSF, plasma, serum, urine, iPSCs) and clinical data to the research community. Information on available biosamples can be found at www.michaeljfox.org/biosamples and data can be found at www.michaeljfox.org/datasets. Visit us at Booth #2030 in the non-profit section to speak with us about these available resources and our funding programs.